NeuroImage: Clinical 12 (2016) 1004–1012

Contents lists available at ScienceDirect

NeuroImage: Clinical

journal homepage: www.elsevier.com/locate/ynicl

Functional resting-state fMRI connectivity correlates with serum levels of the S100B protein in the acute phase of traumatic brain injury☆

William Hedley Thompson[a], Eric Peter Thelin[a], Anders Lilja[c], Bo-Michael Bellander[a,b], Peter Fransson[a,*]

[a]Department of Clinical Neuroscience, Karolinska Institutet, Stockholm, Sweden
[b]Department of Neurosurgery, Karolinska University Hospital, Stockholm, Sweden
[c]Section of Neuroradiology, Department of Clinical Neuroscience, Karolinska Institutet, Stockholm, Sweden

ARTICLE INFO

Article history:
Received 11 October 2015
Received in revised form 21 April 2016
Accepted 5 May 2016
Available online 9 May 2016

Keywords:
Traumatic brain injury
Resting-state
Brain connectivity
fMRI
S100B

ABSTRACT

The S100B protein is an intra-cellular calcium-binding protein that mainly resides in astrocytes in the central nervous system. The serum level of S100B is used as biomarker for the severity of brain damage in traumatic brain injury (TBI) patients. In this study we investigated the relationship between intrinsic resting-state brain connectivity, measured 1–22 days (mean 8 days) after trauma, and serum levels of S100B in a patient cohort with mild-to-severe TBI in need of neuro-intensive care in the acute phase. In line with previous investigations, our results show that the peak level of S100B acquired during the acute phase of TBI was negatively correlated with behavioral measures (Glasgow Outcome Score, GOS) of functional outcome assessed 6 to 12 months post injury. Using a multi-variate pattern analysis-informed seed-based correlation analysis, we show that the strength of resting-state brain connectivity in multiple resting-state networks was negatively correlated with the peak of serum levels of S100B. A negative correspondence between S100B peak levels recorded 12–36 h after trauma and intrinsic connectivity was found for brain regions located in the default mode, fronto-parietal, visual and motor resting-state networks. Our results suggest that resting-state brain connectivity measures acquired during the acute phase of TBI is concordant with results obtained from molecular biomarkers and that it may hold a capacity to predict long-term cognitive outcome in TBI patients.

1. Introduction

Traumatic brain injury (TBI) is the most common cause of death up to 40 years of age (Jennett, 1996). For survivors, TBI may lead to long term cognitive disabilities that can persist for several years after trauma (Miller, 1966; Dikmen and Reitan, 1978; van Zomeren and van den Burg, 1985). Even in cases deemed to be less severe, it has been shown that impairments of cognitive and emotional functions can remain for over a decade (Draper et al., 2007; Draper and Ponsford, 2008). In a time perspective that stretches for up to 30 years, it has been reported that impairment in cognitive function is qualitatively different, albeit with a large within-group variability (Himanen et al., 2006). The collective burden on society related to TBI related injuries is further exacerbated by the long-terms effects from socio-economic factors such as unemployment and dysfunctional relations (Temkin et al., 2009). The World Health Organization (WHO) estimates that TBI will be the most common reason why people are living with a disability by the year 2020 (World Health Organization. Projections of Mortality and Burden of Disease to 2030: Deaths by Income Group. Geneva; 2002 12/01/06). It is therefore of paramount interest to find strategies based on neurological biomarkers that can accurately predict the functional outcome after TBI as well as to design individualized treatment plans to facilitate recovery processes that lead to improved long-term cognitive performance.

To this end, predicting the degree of functional impairment following brain trauma has proven to be a challenging task. Long-term functional outcome in TBI can be assessed using different scales, where the Glasgow Outcome Score (GOS) is the most common (Jennet and Bond, 1975). At the scene of accident and at admission to the hospital, the severity of TBI is commonly assessed using the Glasgow Coma Scale (GCS) (Teasdale and Jennett, 1974; Stocchetti et al., 2004; Husson et al., 2010). Other predictors of long-term functional outcome after TBI include age (Miller et al., 1981; Hukkelhoven et al., 2003; Mushkudiani et al., 2007; Vos et al., 2010), computerized tomography (CT) scans of the head (Maas et al., 2005) and pupil responsiveness (Marmarou et al., 2007; Martins et al., 2009). However, even when factors are combined, it has been shown to be an insufficient means to provide an accurate assessment of long-term functional outcome. Only a small portion (3.5–6%) of the variance in outcome can be accurately modeled (Murray et al., 2007). In the acute phase, relevant information regarding the progression of pathology caused by TBI may also be obtained from a examining the concentration of biomarkers found in serum levels (Yokobori

☆ Conflict of interest: None.

* Corresponding author.
E-mail address: Peter.Fransson@ki.se (P. Fransson).

http://dx.doi.org/10.1016/j.nicl.2016.05.005

et al., 2013). The most studied biomarker of brain injury is the predominantly astrocytic, neurotrophic protein S100B (Donato et al., 2009). In the context of brain injury, levels of S100B in serum have been directly correlated to the extent of cerebral parenchymal damage (Pleines et al., 2001), which have led to several clinical applications (Astrand et al., 2013) including screening for patients eligible for CT scanning in the emergency room (Undén et al., 2013), monitoring unconscious patients in the neuro-intensive care unit (Thelin et al., 2014; Raabe et al., 2004) and as an outcome predictor in severe TBI (Ingebrigtsen et al., 1995; Raabe et al., 1999; Hermann et al., 2000). Interestingly, recent research has shown that the highest serum level of S100B sampled within 12–36 h after trauma could explain a significant additional amount of variance in excess of known outcome parameters, including age, GCS, pupil reaction and computerized tomography measures, as earlier levels might be affected by extracranial contributions (Thelin et al., 2013).

Recently, there has been an increased interest to utilize resting-state fMRI brain connectivity measures to assess the link between brain damage and cognitive function in TBI (for a recent review, see Ham and Sharp, 2012). The majority of previous resting-state fMRI studies have focused on the integrity of the brain's large-scale fMRI connectome in the chronic phase of TBI compared to healthy controls (e.g. Nakamura et al., 2009; Kasahara et al., 2010). Differences in brain connectivity compared to healthy controls have primarily been reported in the default mode (DM) network (Hillary et al., 2011; Sharp et al., 2011), fronto-parietal (Hillary et al., 2011), salience (Bonnelle et al., 2012) and motor networks (Kasahara et al., 2010). Additionally, graph theoretical approaches applied to brain network connectivity patterns have revealed a reduced degree of small worldness in TBI patients (Pandit et al., 2013). Recently, investigations that address brain connectivity during the acute phase of TBI have been reported (Shumskaya et al., 2012; Iraji et al., 2015; Mayer et al., 2015).

The main objective of this study was to investigate whether differences in resting-state fMRI connectivity measured during the acute phase of TBI correlates with serum levels of S100B sampled during the acute phase of TBI. Given previous research on the relationship between S100B levels and long-term GOS ratings, a finding of a correspondence between serum levels of S100B and resting-state brain connectivity would suggest that that resting-state connectivity acquired during the acute phase has to some extent a predictive capacity for the long-term functional outcome after TBI. In a cohort of 24 patients with mild to severe TBI, resting-state fMRI data was acquired during sedation at an average time-point of 8 days post-injury. Due to the heterogeneity of the brain damage, we opted to use a multivariate-pattern analysis (MVPA)-informed analysis of resting-state fMRI data at the cohort level to extract seed points of interest for whole-brain brain connectivity analysis. Our main hypothesis was that higher serum levels of S100B in the acute phrase of TBI is accompanied by an overall weaker functional connectivity resting-state network structure in the brain.

2. Materials and methods

2.1. Patient data, sampling of S100B and MRI scanning procedure

Twenty-four patients (age range: 16–67 years; mean 36.7 years) with traumatic brain injury in need of neuro-intensive care were included in this study (approved by the Stockholm county ethical committee; #2010/1072-31/1). Inclusion of patients in the study was dependent on the availability of author BMB. The severity of head injury was assessed using the Glasgow Coma Scale (range = 3–14, mean = 8.4) at first contact with medical staff. Between 1 and 22 days after admission to the neurointensive care unit at the Karolinska Hospital in Stockholm, patients underwent an MRI examination (1.5 T Siemens, Erlangen, Germany). The anatomical MRI protocol was tailored for imaging in trauma and included sequences as diffusion-weighted imaging and FLAIR. Additionally, we acquired susceptibility-weighted images (SWI), originally described in clinical work by Haacke and colleagues (Sehgal et al., 2005), which have a high sensitivity for hemorrhagic components in various lesions and a several-fold superior to previous imaging techniques. The SW-imaging sequence thus has been increasingly used in the characterization of traumatic hemorrhages and of venous vasculature, especially in finding micro-hemorrhages in axonal injuries (Wintermark et al., 2015). In addition to anatomical MR imaging, resting-state fMRI data were collected (TR / TE = 2500 / 40 ms, flip angle = 90 degrees, voxel size = 2x2x2 mm^3, number of image volumes = 200). Functional outcome was assessed between 6 and 12 months after the time-point of injury using the Glasgow Outcome Scale (GOS) from either clinic visits or from questionnaires sent to the patients. The latest assessed GOS were used in the study (GOS = 1 – death, GOS = 2 – persistent vegetative state, GOS = 3 – dependent, severe disability, GOS = 4 – independent, moderate disability, GOS = 5 – recovered, low disability). Two patients died (GOS = 1), five patients displayed severe disability (GOS = 3), ten moderate disability (GOS = 4) and seven patients showed low disability (GOS = 5) (Jennett and Bond, 1975. We also included the number of days after trauma that outcome was noted. During the acute phase, all patients were given sedatives (midazolam, propofol, morphine) and/or vasoactive drugs (dobutamine, noradrenaline, catapressan, nimotope, ephedrine). The two patients that scored GOS = 1 were excluded from the analysis since the imaging data from the first patient could not be retrieved whereas images from the second patient could not be preprocessed accurately. Additionally, data from one other patient was excluded from the analysis due to difficulties with the co-registration and normalization of the MR imaging data due to extensive anatomical pathology. Thus, data from 21 patients were included in the analysis. For the 21 patients, the number of days between admission to the NICU and MRI examination varied between 1 and 22 days. A full account of all drugs administered and other relevant clinical data is given in Supplementary Table S1 and the neuro-radiological findings for all patients are described in Supplementary Table S2.

2.2. Treatment

The neurosurgical department at Karolinska University Hospital adheres to guidelines similar to those set forth by the Brain Trauma Foundation (Brain Trauma Foundation et al., 2007). Unconscious TBI patients are intubated and mechanically ventilated. Intracranial mass lesions are evacuated as deemed appropriate by the attending neurosurgeon. Severe TBI patients (GCS = 3–8) are monitored via extraventricular drains or intraparenchymal pressure devices to monitor intracranial pressure (ICP) which is targeted at <20 mmHg using sedation, osmotic therapy and, if necessary, mild hypothermia and pentobarbital infusion (surveilled using continuous EEG). Central perfusion pressure (CPP), calculated as mean arterial pressure (MAP) – ICP, is targeted at >50 mmHg and the pressure reactivity index is used to guide treatment. Intraparenchymal microdialysis and oxygen saturation devices are used in selected patients to improve cerebral monitoring. MRI is performed in all severe TBI patients, as well as in patients that exhibit signs of diffuse axonal injury (DAI), when deemed clinically stable enough to be transported from the NICU.

2.3. S100B analyses

At our institution, as part of our clinical routine, we sample S100B from arterial blood twice daily (06:00 AM and 06:00 PM) in all patients in the NICU. Since 2008, the department of clinical chemistry at Karolinska University Hospital use the electrochemiluminescence assay Elecsys (Roche Diagnostics, Basel, Switzerland) to immediately analyze the serum samples. The peak level 12–36 h after injury was acquired as it has been shown to best correlate to long-term functional outcome (Thelin et al., 2013). Moreover, if a secondary peak of S100B after 48 h was detected it was noted, as these increases have been

shown to correlate to the development of secondary intracranial injuries (Thelin et al., 2014).

2.4. Clinical parameters

Pre-hospital GCS, hypoxia, hypotension and presence of epileptic seizures were acquired from pre-hospital trauma charts. These were also used to assess trauma time, which was defined as the time when the emergency call reached the alarm central. GCS (GCS 3–8 = severe TBI, 9–13 = moderate TBI and 14–15 = mild TBI (Teasdale and Jennett, 1976)) and pupil responsiveness were acquired using hospital charts. The motor score in GCS has been shown to be the best predictor of outcome and was thus analyzed separately (Ross et al., 1998). Head abbreviated injury score (AIS) (Greenspan et al., 1985) was assessed at admission to the hospital, as well as injury mechanism, presence of major extracranial trauma and energy during accident as defined by Advanced Trauma and Life Support (ATLS) guidelines (ACS, 2012). Weight was measured at the arrival to the NICU. At the timing of the performed fMRI, the dosage of drugs, blood pressure, ICP and CPP were noted form anesthetic charts (if available). Newcastle Sedation Score, as assessed by NICU nurses (range 4–19, where 4 denote anesthetized and 19 is fully awake, see also Cook and Palma, 1989) from the day of MRI examination, was acquired from electronic hospital charts. Further details can be found in Supplementary Tables 1 and 2.

2.5. fMRI data analysis

In each patient, 8 min 30 s (510 s) of resting state fMRI data was recorded. Image preprocessing and resting-state fMRI connectivity analysis was performed in the SPM8 software platform (Friston et al., 1995), CONN toolbox v14.k (Whitfield-Gabrieli and Nieto-Castanon, 2012) and Matlab (Mathworks Inc., MA, USA). The first four scans (10 s) were not used in the analysis, leaving 500 s worth of data per patient. Image preprocessing steps included anatomical segmentation, normalization to MNI (Montreal Neurological Institute) space, spatial smoothing (FWHM = 8 mm), band-pass filtering (0.01–0.1 Hz) and regressing out signal contributions from head motion, white matter and cerebrospinal fluid (Whitfield-Gabrieli and Nieto-Castanon, 2012). Signal contributions from micro head-movements were accounted for using the image "scrubbing" (Power et al., 2011) ART method as implemented in the CONN toolbox. Notably, due to sedation, the number of scrubbed images was very small (using a frame-wise displacement (FD) threshold of 0.5). Finally, resting-state BOLD signal intensity time-courses were detrended. The combination of drugs administered, reduced by correspondence analysis (see below), and age were used as nuisance regressors in the group level analysis.

It is well-known that sedative drugs such as propofol and midazolam influence the strength of resting-state functional brain connectivity (Greicius et al., 2008; Boveroux et al., 2010; Schrouff et al., 2011). In the present study, the type and combination of anesthetics used in acute phrase was based on clinical considerations at the individual level. Therefore, a mixture of different sedative drugs was administered during the acute phase (see Supplementary Table 1 for a full account of anesthetics used. Note that the data tabulated in Supplementary Table 1 are the drugs administered at the time-point of MRI data acquisition). To minimize the influence from sedation on the brain connectivity results, model regressors at the group level were created to account for data variability related to the mixture of sedative drugs given. However, since the size of studied cohort was rather small and the categorical data representing the mixture of drugs given was large, the risk of overfitting the data with nuisance variables was deemed to be substantial. To alleviate the potential problem of model overfitting, we employed a correspondence analysis (CA, Greenacre, 1983) to reduce the dimensionality of the nuisance (sedation) variable space from nine categorical to four continuous regressors (Lorenzo-Seva et al., 2009). CA is a mathematical tool that reduces the dimensionality of data and it can be viewed as the categorical variable version of the independent component analysis (ICA) that handles continuous data. The reduced dimensionality of four was chosen as the four dimensions was the smallest number of regressors that together explained more than the averaged regressor. Thus, the four regressors derived from the correspondence analysis together with an additional age-regressor were used in the 2nd level analysis on brain connectivity at a group level (see also Supplementary Fig. S1 for a graphical representation of the Correspondence Analysis).

Although region-of-interest (ROI) based correlation analysis has been successfully used in many clinical studies of resting-state connectivity showing abnormal connectivity patterns within pre-selected networks (for a review, see Fox and Greicius, 2010), seed ROI correlation analysis performed in cohorts harboring a considerable degree of inhomogeneity in terms of location and extent of brain damage such as the present cohort is not straightforward. The practice of a-priori selection of ROIs as seed points for a connectivity analysis, although it is often defined so that it aims to target the functional brain anatomy of a-priori defined resting-state networks, will inevitably lead to an experimental disadvantage in terms of a user selection bias in anatomical specificity. This problem, we believe, might be further amplified in the present cohort that include a strong inherent diversity in localization as well as severity of pathological processes due to hemorrhages, contusions as well as more subtle damage caused by diffuse axonal injuries (DAI).

Hence, to mitigate the effects from this potential problem in our analysis pipeline, we opted to use a data-driven, multi-variate pattern analysis (MVPA) as implemented in the "connectome-MVPA" CONN toolbox (Whitfield-Gabrieli and Nieto-Castanon, 2012) to find suitable seed-regions for analysis of brain connectivity during acute TBI. The method has been used in several recent studies (Whitfield-Gabrieli et al., 2015; Beaty et al., 2015). The aim of this method is to derive seeds based on the data prior to performing a post hoc analysis on the seeds to analyze brain connectivity patterns. The MVPA method computes functional connectivity patterns for each voxel by performing a principal component analysis (PCA) on the connectivity patterns between each single voxel to all other voxels. For a given voxel, *vi*, a PCA is performed by retaining c number of components (c = 3, see below), across all subjects, between *vi*'s connectivity with all other voxels. In other words, each voxel has a c-dimensional representation of the spatial pattern of its connectivity to all other voxels for each subject. Thereafter, an omnibus test was carried out comparing the between-subject variance in relation to S100B peak levels performed across all voxels' connectivity patterns in c-dimensional space. The reduced sedation regressors (by means of Correspondence Analysis) and age were used as nuisance regressors. This test gives clusters of voxels that displayed a similar between-subject variance of their spatial connectivity. The results were thresholded at cluster size ($k > 100$ voxels) and peak value ($p < 0.05$, uncorrected). This resulted in 4 clusters, which were used as seeds points of interest in a post-hoc analysis of brain connectivity. Further, a whole-brain post hoc ROI-based connectivity analysis was carried out for the four derived clusters against all other voxels in the brain, testing which areas of the brain changes its connectivity in relation to S100B peak serum levels. For each of the seed ROIs, the four sedation regressors and an age regressor were used as co-variates of no interest. Statistical parametrical connectivity maps were thresholded at the voxel level of $p < 0.001$, uncorrected, two tailed and at the cluster level of $p < 0.05$ FDR corrected. Of note, for the employed MVPA method, one parameter had to be chosen, namely the number of PCA components kept for each voxel, which was here set to 3. This choice was motivated by convention where c is equal to 10–20% of the number of subjects (which here falls between 2 and 4). Assignment of resting-state network membership for each significant cluster of brain connectivity provided in Tables 1 and 2 was done using the www.neurosynth.org meta-analysis online tool (Yarkoni et al., 2011).

Table 1
Seed regions derived from the multi-variate pattern analysis of resting-state fMRI data of all subjects included in the study. Anatomical coordinates for the seed regions are given in the MNI (Montreal Neurological Institute) format together with its corresponding location in the AAL atlas (Automated Anatomical Labeling, Tzourio-Mazoyer et al., 2002), assigned resting-state network, cluster size (k) and p-value (uncorrected at cluster level $p < 0.05$ for $k > 100$).

Cluster Coordinates (MNI)			Location (AAL)	Network	k	p-uncorrected
14	−70	62	Precuneus R	Default mode	301	0,00024
−38	−42	−46	Cerebellum 8 L	Sensorimotor	234	0,00082
36	−72	50	Angular R	Fronto-parietal	221	0,00106
−38	−52	60	Parietal Sup L	Parietal-premotor	116	0,01066

2.6. Assessment of image regions with insufficient BOLD contrast due to trauma

In order to assess whether our connectivity results were influenced by poor underlying BOLD signal contrast resulting from localized trauma, we constructed an approximate group brain lesion maps based on the following procedure. First, we located voxels that had a probabilistic value above 70% of being residing in gray matter based on the SPM8's a-priori gray matter mask. This ensured that we were assessing brain voxels that could potentially contain a BOLD signal that originated from gray brain matter. Second, in each subject, we calculated the average BOLD fMRI signal for each voxel in the normalized (but spatially unsmoothed) images, masked by SPM8 a-priori gray matter template. If the BOLD signal intensity for a given voxel was below 2 standard deviations, it was marked as "bad". Bad voxels were summed over subjects and displayed in Supplementary Fig. S2, along with the seeds and connectivity results. Note that a voxel marked as bad is not necessarily a voxel that is affected by the trauma, but are voxels with relatively less BOLD signal than other voxels (which is to be expected at trauma locations). The lesion map offers an approximation of possible (but not definitive) lesion voxels and thus is helpful for comparing brain connectivity results in relation to the anatomical localization of lesions.

3. Results

3.1. Anatomical and clinical findings

The included patients were in general males (see Supplementary Table 1). Almost half suffered from major extracranial trauma and falls were the most common injury mechanism. Even if some patients were conscious at admission to the hospital (GCS range of 3–14), a majority suffered from severe-to-critical TBI (Head-Abbreviated Injury Score (AIS) 4–5). With regard to morphological brain lesions, an overview of their types, location and numbers can be found in the Supplementary Table 2. Traumatic axonal injuries (TAI) were (by definition) distributed in white matter, mostly subcortically, less often in deeper regions, and in four patients also present in the brainstem. Lesions of TAI type in basal ganglia or thalamus were seen in a few subjects. These TAIs were predominantly hemorrhagic, and only remarkably few of these patients demonstrated TAIs as merely diffusion abnormalities or visible on FLAIR images. Cortical lesions bearing the characteristics of contusions were seen in almost all patients.

3.2. The relationship between S100b peak values and intrinsic functional brain connectivity

The MVPA analysis revealed four significant clusters located in the right precuneus, left cerebellum, right angular gyrus and in the left superior parietal gyrus. The spatial localization of the four brain clusters identified using the multi-variate pattern analysis is displayed in Fig. 1 and tabulated in Table 1. Next, we focused on the four brain clusters that displayed a MVPA-derived variability in brain connectivity tied to the peak levels of S100B. We performed four separate seed-based whole-brain correlation analysis of the resting-state fMRI data and corrected for multiple comparisons at cluster level (peak level: $p < 0.001$, uncorrected; cluster level: $p < 0.05$ FDR-corrected). For all four tested seed regions, we found a negative correlation between the level of S100B and the strength of brain connectivity. Brain regions that showed significant differences in brain connectivity related to serum levels of S100B is shown in Fig. 2 and the statistical results together with the corresponding anatomical coordinates are presented in Table 2. The seed region located in the right precuneus was found to be negatively correlated with the visual, motor and the mid-line section of the default mode network as a function of S100B levels. Similarly, the strength of connectivity between the seed brain region positioned in the left cerebellum (lobule VIII) and brain regions located in the visual, auditory, and fronto-parietal networks were negatively coupled to S100B levels. Moreover, the seed region situated in the right angular gyrus showed a negative connectivity with brain nodes located in the visual and default networks. Finally, the seed region in the right superior parietal lobule was negatively correlated with the sensorimotor part of the cerebellum and visual network as a function of the S100B serum level.

The connectivity between the precuneus seed region and the visual network, the angular gyrus seed region and the DM network and visual network as well as the connectivity between the parietal seed region and the visual network survived a further multiple comparison

Table 2
Brain connectivity results for each seed region (tabulated in Table 1). Results were thresholded at peak level $p < 0.001$ (uncorrected) and $p < 0.05$ at cluster level (FDR corrected). An asterisk indicates that the connectivity result survived a Bonferroni correction (taking into account that four brain seed regions were tested).

	Peak coordinates (MNI)			Location (AAL)	Network	k	T-value	p-FDR
Precuneus R	−26	−84	18	Occipital Mid L	Visual	212	−6,68	0,00307*
	−2	−40	32	Cingulum Post L	Default mode	136	−6,31	0,01259
	2	−78	32	Cuneus L	Visual	82	−5,60	0,04412
	24	32	38	Frontal Mid R	Default mode	82	−9,09	0,04412
	−32	−6	60	Precentral L	Pre/Motor	76	−5,41	0,04551
Cerebellum 8 L	−10	−78	26	Cuneus L	Visual	140	−7,24	0,01553
	−22	22	68	Frontal Sup L	Frontal-parietal	117	−7,25	0,01726
	60	−16	−8	Temporal Mid R	Auditory	89	−7,37	0,03463
	−32	−82	−24	Cerebellum Crus1 L	Supramodal	80	−6,47	0,03526
	36	−74	18	Occipital Mid R	Visual	77	−7,03	0,03526
	0	−78	2	Lingual L	Visual	73	−5,71	0,03538
Angular R	10	−48	30	Cingulum Post R	Default mode	931	−7,20	0,00002*
	56	−52	24	Temporal Sup R	Default mode	196	−6,15	0,00254*
	40	−78	22	Occipital Mid R	Visual	141	−5,30	0,00797*
	−18	−90	36	Occipital Sup L	Visual	93	−5,58	0,03151
Parietal Sup R	−18	−82	42	Occipital Sup L	Visual	751	−8,96	0,00003*
	14	−84	−32	Cerebellum Crus2 R	Supramodal	101	−11,27	0,04965

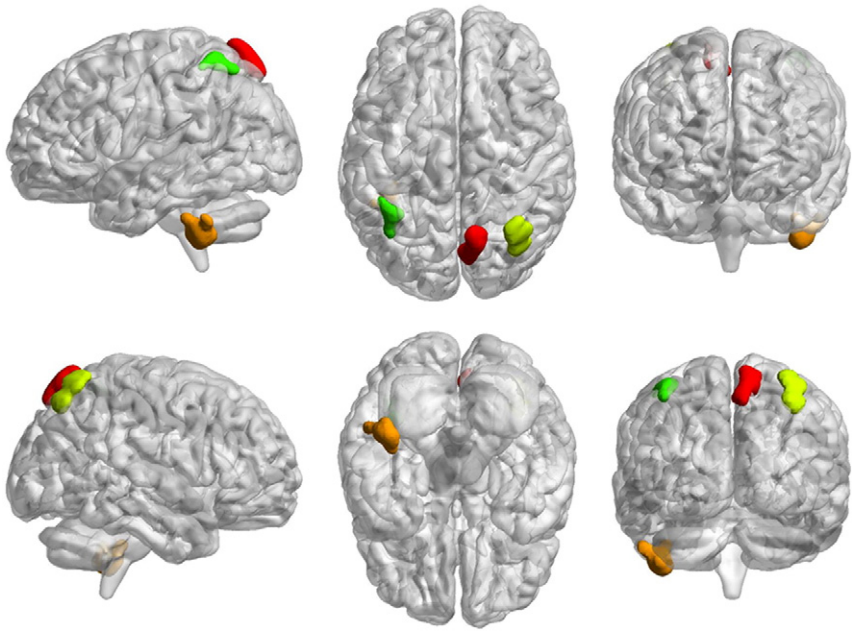

Fig. 1. The anatomical localization of the four seed region-of-interest obtained from the multi-variate pattern analysis is shown in sagittal, axial and coronal orientations. Clusters were found in Preceneus R (Red), Cerebellum L (Orange), Angular R (yellow); Parietal Sup. R (green) ($p < 0.05$, uncorrected, cluster size $k > 100$).

Bonferroni correction for the four tests performed. Graphs that show the degree of connectivity between brain regions and S100B serum levels that survived the Bonferroni correction are shown in Fig. 3 where the final GOS outcome of the patients has also been added for illustrative purposes. It is noteworthy that the opposite contrast, i.e. strength of brain connectivity that scales positively with higher S100B levels, yielded no significant results.

4. Discussion

First, it should be borne in mind that several previous investigations using large sample cohorts have shown robust experimental evidence for a relationship between long-term functional outcome and high S100B levels during the acute phase of TBI (Thelin et al., 2013; Mercier et al., 2013; Thelin et al., 2014). Our main finding was that for all brain regions examined in the acute phase of brain injury, the connectivity profiles for a multitude of large-scale resting-state networks were found to be diminished in strength as a function of the sampled serum levels of S100B, a biomarker for neuronal damage. For the two seeds regions located in the precuneus and angular gyrus, we could detect a reduced degree of resting-state brain connectivity with the posterior cingulate cortex, medial prefrontal cortex and right superior temporal cortex. Hence, a decreased strength of within-DM network connectivity was present that correlated with increased levels of S100B, suggesting that the severity of TBI estimated by S100B serum levels is related to the uninterrupted flow of neuronal information within the DM network. It is of interest to compare our findings regarding the function of the DM network in TBI patients with previous research that have targeted DM network during the chronic phase. The notion that the integrity of the DM network is of importance for TBI have gained support from both resting-state as well as task-based fMRI studies in chronic TBI patients. By employing a choice reaction time task, Bonnelle et al., 2011 showed that attentional deficits in TBI patients correlated with increases in brain activity in the posterior cingulate cortex and medial prefrontal cortex, both of which are key hubs in the DM network (Fransson and Marrelec, 2008; Buckner et al., 2008). Moreover, the same research group has reported of an increased risk of failure to deactivate the DM network in TBI patients during an inhibitory control condition such as the Stoop task (Bonnelle et al., 2011). In a notable study, Hillary et al., 2011 reported increased within-DM network connectivity in a longitudinal (6 versus 3 months post-injury) study of patients with moderate-to-severe TBI. In a similar vein, a recent study in TBI patients in the chronic phase showed that the degree of within-DM network connectivity were higher in patients which had the least cognitive impairment (Sharp et al., 2011). Hence, previous results speak to the fact that there exist ample experimental support for the idea that a reduction in the capacity for neuronal communication within the DM network in the chronic phase of TBI leads to a decline in cognitive outcome.

The current study on intrinsic brain connectivity is in agreement with two recently published studies that focused on the acute phase of TBI. For patients with mild TBI (GCS = 13–15) scanned using rs-fMRI during the acute phrase, a reduced functional connectivity in the DM compared to healthy controls was reported (Iraji et al., 2015). The reduced connectivity was in particular observed in the posterior hub of the DM, the medioparietal cortex encompassing the posterior cingulate cortex and the precuneus. Similarly, in a study encompassing forty-eight patients with mild TBI, resting-state ICA fMRI connectivity analysis carried out in the semi-acute phase (mean = 14 days post-injury), Mayer and colleagues found a reduced pattern of within-DM connectivity compared to healthy controls, albeit at an uncorrected threshold (Mayer et al., 2015).

To the best of our knowledge, the current study is the first functional neuroimaging study that has investigated the relationship between the serum levels of an astrocytic biomarker (S100B, sampled 12–36 h post-injury, see Materials and methods) and resting-state brain connectivity in the acute phase of TBI. The general finding of an overall negative relationship between resting-state brain connectivity, particularly so for the DM network, and serum levels of S100B is a promising result in terms of the abiding long-term goal of combining imaging data with molecular markers to facilitate the capability to predict the long term functional outcome in TBI. In this context it is worthwhile to point out that a recent study conducted in 265 mild-to-severe TBI patients could show a robust relation between levels of S100B in serum and functional outcome estimated with GOS (Thelin et al., 2013). Moreover, the same study presented statistical evidence that S100B levels had a stronger univariate relation to cognitive outcome than many known important TBI predictors such as age, pupil response, GCS and Computerized Tomography (CT) values. Importantly, the study by Thelin et al. (2013)

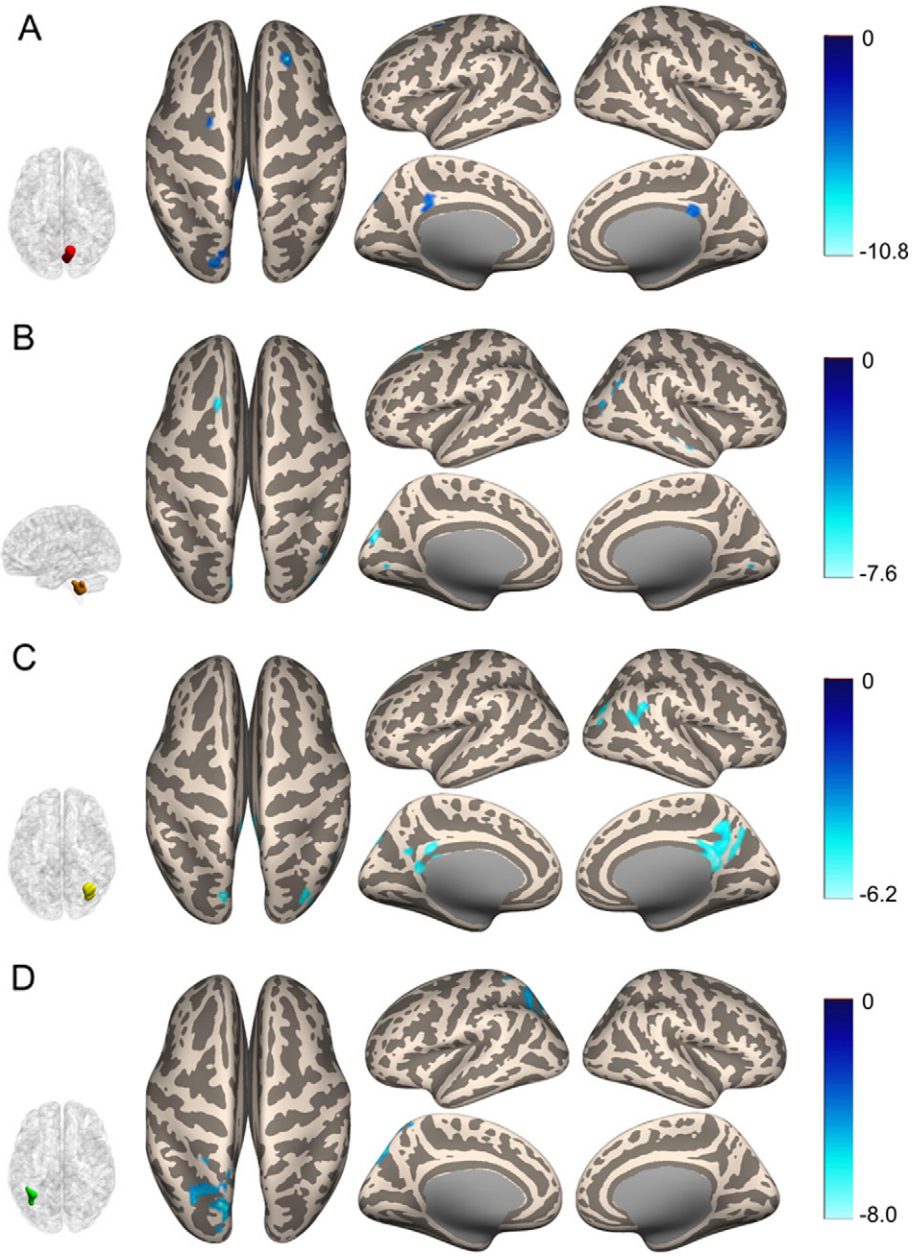

Fig. 2. Results from the resting-state brain connectivity analysis. The left column shows the anatomical localization of the brain seed regions used in the connectivity analysis (see also Fig. 2). The middle and right columns shows brain regions that were significantly negatively correlated ($p < 0.001$, two-sided; cluster level: $p < 0.05$, FDR-corrected) with S100B serum levels for the four seeds (interpolated onto a smooth surface of the brain). Further information regarding the clusters is given in Table 2.

showed the predictive power of S100B remains even in a multivariate analysis, contributing >6% partial R^2 to the multivariate prediction models. Thus, the previous data on the S100B biomarker together with the brain connectivity/S100B results presented in the current study suggests that assessments of long term cognitive outcome after TBI might prove to be of value if both resting-state fMRI and sampling of S100B are performed during the acute phase.

Since we for all included patients had collected data pertaining to the GOS ratings between 6 and 12 months post injury, it is a valid question to ask why resting-state brain connectivity was not regressed against GOS ratings and thus complement the presented analysis with an assessment of the correspondence between rs-fMRI brain connectivity and GOS ratings. There are several reasons for why we opted to refrain from carrying out this correlation analysis. The patients included in the present fMRI analysis were unevenly distributed among the three possible GOS categories (GOS = 3–4 patients; GOS = 4–10 patients, GOS = 5–7 patients). The skewness in the rating distribution among the three GOS categories is not optimal from a statistical point of view and could potentially lead to biased results.

The fact that the observed correlation between S100B serum levels and decreases in resting-state connectivity was not exclusively found within the DM network, but rather also included visual, auditory, sensory and fronto-parietal networks is not overly surprising given the heterogeneity of localization of brain damage in the examined cohort of examined patients. Additionally, as outlined in Supplementary Table 2, anatomical MR scans revealed in several patients a presence of diffuse axonal injuries (DAI) that are known to cause impairment in cognitive outcome (Scheid et al., 2003; Moen et al., 2014). Although DAI injuries can be readily visualized as microbleeds in T2*-weighted MR scans, as alterations in diffusion-weighted images or displayed in e.g. FLAIR imaging, there are good reasons to believe that far from all DAI related injuries are detected in MRI at a given time-point, especially as the

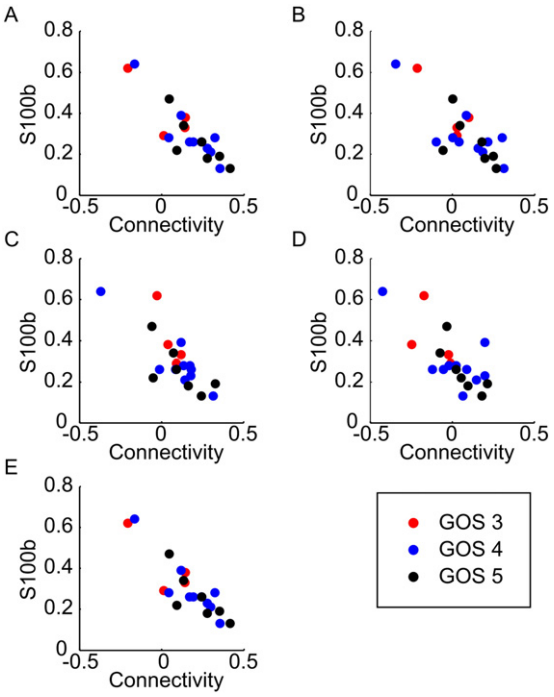

Fig. 3. Strength of brain connectivity and S100B serum levels for the five brain clusters that survived Bonferroni correction ($p < 0.05$, see also Table 2). Additionally, for each patient the corresponding Glasgow Outcome Scale (GOS) value given in a color-coding scheme (GOS3 = red, GOS4 = blue, GOS5 = black). Panel (A) shows the brain connectivity relationship between the right precuneus and left middle occipital gyrus and S100b serum levels, (B) right angular gyrus – right PCC, (C) right angular gyrus – right superior temporal gyrus, (D) right angular gyrus – right middle occipital gyrus and (E) right superior parietal lobule – left superior occipital cortex.

diffusion characteristics seem to change during the acute-subacute phase. Interpreting the spatial distribution of inflicted resting-state networks in relation to morphological changes thus warrants further caution.

Although the size of the cohort analyzed in the present study was sufficiently large to show significant results regarding the relationship between S100B peak levels and the overall patterns of strength of intrinsic brain connectivity, it was deemed inadequate in size to allow for a specific assessment of the location of brain damage versus the effect on resting-state network connectivity. We foresee that in future studies that include substantially larger cohorts, we will be able to make progress towards the aim of a stratification system between the spatial distribution of white and gray matter damage and the specifics of intrinsic resting-state network connectivity at an individual level (Irima et al., 2012). A limitation of S100B is that levels are correlated to cerebral lesion size, independent of localization of injury (Pleines et al., 2001). Obviously, a contusion or other lesion, even if small in size, in a more critical part of the cerebral network would more severely affect brain connectivity and presumably not be accurately represented by the S100B level. In patients with only diffuse cerebral injuries, lower levels of S100B are usually present (Chabok et al., 2012). However, we included S100B levels sampled 12 h after injury, as earlier samples are more heavily influenced by extracranial trauma (Thelin et al., 2015) and we could not detect any correlation between age, gender and multitrauma with our levels of S100B (data not shown), hence proving its role as a marker of intracranial injury. Another limitation of the current study is that resting-state fMRI data were acquired during anesthesia. As discussed earlier, anesthetics such as propofol and midazolam result in a general decrease in intrinsic brain connectivity. Moreover, it has been reported that networks encompassing frontal, temporal and parietal brain areas were relatively more affected by propofol than primary sensory regions (Schrouff et al., 2011). Similarly, it has been shown that mild sedation using midazolam reduces within-default mode network connectivity (Greicius et al., 2008). Thus, although we took measures to account for differences in administration of sedative drugs in the analysis using regressors constructed via correspondence analysis, it cannot be ruled out that the effects of sedation might play a role in terms of resting-state networks involved. Another limitation is the heterogeneity of our cohort, comprising of mild-to-severe TBI cases (see Supplementary Table S1). TBI severity has historically been categorized using GCS, however GCS has obvious limitations in its subjectivity (Bledsoe et al., 2014) and the fact that the patients may be sedated (Stocchetti et al., 2004). In the current study, TBI patients in need of neuro-intensive care for their head injuries were included which we believe represents a clinically valid and reproducible cohort of TBI patients and as can be seen by the AIS, all suffered from structural severe TBI. GOS has been criticized for being too crude in its assessment of outcome, hence a new 8-grade scale GOS extended (GOSE) has been introduced (Teasdale et al., 1998). Moreover, there are other assessment scales for cognitive-, motor- and memory functions as well as depression following TBI (Tate et al., 2013). While we have recently introduced GOSE, which is considered the golden standard for functional outcome following TBI, we unfortunately do not have any other assessments available for these patients. However, we do not believe this to be a major limitation because even if it would be good to better assess outcome, it would introduce a methodological and statistical problem how to aggregate to outcome data. The result would probably have been that we would have used GOS, which is also due to the limited sample size in the current study. Moreover, as can be seen, the GOS was assessed at similar time-points for all patients (Supplementary Table 1). There is today no clear consensus when to assess GOS. Six months have been suggested by many, but improvement is possible in up to 15 months following injury (Miller et al., 2005) thus our time point of approximately 12 months falls within this time period.

Moreover, due to fact that the exact anatomical localization of brain lesions varied between subjects in the examined cohort, it is a valid question to ask whether the inhomogeneity of lesions, with the accompanying signal loss in the BOLD fMRI signal images, might have influenced the connectivity results. To show that this was not a cause for concern, we computed an approximate anatomical map of brain lesions across all subjects, shown in Supplementary Fig. S2 (see also Materials and methods section). From the lesion map shown in Supplementary Fig. S2 we can observe that voxels residing in locations of suspected lesions (a.k.a. "bad" voxels) are in almost all cases anatomically separated from seed volumes as well as from significant clusters of brain connectivity. Specifically, affected voxels were primarily located in the lateral cerebellum, inferior temporal and occipital lobule and the most ventral part the orbitofrontal cortex. However, the seed volume located in the cerebellum shows to some extent an overlap with bad voxels, but only so for a small portion of the voxels. As previously mentioned in the methods section, voxels labeled as "bad" signifies voxels where the average BOLD fMRI signal intensity was <2 standard deviations below the mean, which should capture most of the voxels affected by brain lesion. However, since the threshold of 2 STD is arbitrarily set, it cannot be ruled out that there are some additional voxels that are influenced by the presence of lesions, although it is unlikely and we believe that our threshold is quite a liberal threshold which may have marked non-lesion voxels as bad. Hence, the maps included in Supplementary Fig. S2 shows that the large majority of the results in terms of brain connectivity changes and their relationship to S100B peak levels are not influenced by regional BOLD fMRI signal loss due to the presence of lesions.

The main strength of our study was that across all seed derived from the MVPA analysis, we found a decrease in intrinsic brain connectivity that correlated significantly with the peak of S100b protein levels in the acute phase of TBI. Differences in connectivity related to the level of S100b were found both within- and between the default mode,

fronto-parietal, motor, visual and auditory networks. The multitude of networks involved reflects that fact that multiple cognitive faculties, such as motor skills, language, attention and social cognition are implicated in the long-term functional outcome after TBI. The present study adds to the growing body of literature that has shown that TBI disrupt neuronal communication in the brain that can be studied at large-scale network level using intrinsic fMRI connectivity. Recent research has provided support for the idea that the effects on the brain after TBI, which commonly include wide-spread diffuse axonal injuries, can be viewed as a network dysfunction disorder (Fagerholm et al., 2015; Fornito et al., 2015; Sharp et al., 2014; Achard et al., 2012). However, it deserves to be noted that when we relate our brain connectivity results to the known resting-state network architecture, we have implicitly assumed the topography of resting-state networks as they typically appear in healthy subjects. Future studies could aim to isolate the specific influence on each resting-state network individually and test for their integrity after TBI, but this poses a methodological challenge due to the heterogeneous nature of brain lesions after traumatic injury.

Although studies in larger cohorts are warranted and would allow for the derivation seed regions and subsequent analysis to exist on separate datasets, our results highlight the potential of using resting-state functional MRI connectivity acquired during the early acute phases of TBI as a biomarker for general functional outcome. In future studies, testing to see whether specific declines in intrinsic connectivity correlate to specific long-term cognitive impairments would entail that resting state fMRI connectivity, combined with molecular biomarkers could be used to identify candidate dys-connections in the large-scale brain connectome that could be targeted in individual treatment plans.

Supplementary data to this article can be found online at http://dx.doi.org/10.1016/j.nicl.2016.05.005.

Acknowledgements

Peter Fransson was funded by the Swedish Research Agency (Vetenskapsrådet), 621-202-4911.

References

Achard, S., Delon-Martin, C., Vértes, P.E., Renard, F., Schenck, M., Schneider, F., Heinrich, C., Kremer, S., Bullmore, E.T., 2012. Hubs of brain functional networks are radically reorganized in comatose patients. Proc. Natl. Acad. Sci. U. S. A. 109, 20608–20613.
ACS, 2012. Advanced Trauma Life Support Program for Doctors. nineth ed. (Chicago).
Astrand, R., Undén, J., Romner, B., 2013. Clinical use of the calcium-binding S100B protein. Methods Mol. Biol. 963, 373–384.
Beaty, R.E., Benedek, M., Barry Kaufman, S., Silvia, P.J., 2015. Default and executive network coupling supports creative idea production. Sci. Rep. 5, 10964.
Bledsoe, B.E., Casey, M.J., Feldman, J., Johnson, L., Diel, S., Forred, W., Gorman, C., 2014. Glasgow coma scale scoring is often inaccurate. Prehosp. Disaster Med. 30, 46–53.
Bonnelle, V., Leech, R., Kinnunen, K.M., Ham, T.E., Beckmann, C.F., De Boissezon, X., Sharp, D.J., 2011. Default mode network connectivity predicts sustained attention deficits after traumatic brain injury. J. Neurosci. 31, 13442–13451.
Bonnelle, V., Ham, T.E., Leech, R., Kinnunen, K.M., Mehta, M.A., Greenwood, R.J., Sharp, D.J., 2012. Salience network integrity predicts default mode network function after traumatic brain injury. Proc. Natl. Acad. Sci. U. S. A. 109, 4690–4695.
Boveroux, P., Vanhaudenhuyse, A., Bruno, M.A., Noirhomme, Q., Lauwick, S., Luxen, A., Degueldre, C., Plenaux, A., Schnakers, C., Philips, C., Brichant, J.F., Bonhomme, V., Maquet, P., Greicius, M.D., Laureys, S., Boly, M., 2010. Breakdown of within- and between-network resting state functional magnetic resonance imaging connectivity during propofol-induced loss of consciousness. Anesthesiology 113, 1038–1053.
Brain Trauma Foundation, American Association of Neurological Surgeons, Congress of Neurological Surgeons, 2007. Guidelines for the management of severe traumatic brain injury. J. Neurotrauma 24 (Suppl. 1), S1–106.
Buckner, R.L., Andrews-Hanna, J.R., Schacter, D.L., 2008. The brain's default network: anatomy, function, and relevance to disease. Ann. N. Y. Acad. Sci. 1124, 1–38.
Chabok, S.Y., Maghadam, A.D., Saneei, Z., Amlashi, F.G., Leili, E.K., Amiri, Z.M., 2012. Neuron-specific enolase and S100BB as outcome predictors in severe diffuse axonal injury. J. Trauma Acute Care Surg. 72, 1654–1657.
Cook, S., Palma, O., 1989. Propofol as a sole agent for prolonged infusion in intensive care. J. Drug Dev. Suppl 2, 65–67.
Dikmen, S., Reitan, R.M., 1978. Neuropsychological performance in posttraumantic epilepsy. Epilepsia 19, 177–183.
Donato, R., Sorci, G., Riuzzi, F., Arcuri, C., Bianchi, R., Brozzi, F., Tubaro, C., Giambanco, I., 2009. S100B's double life: intracellular regulator and extracellular signal. Biochim. Biophys. Acta 1793, 1008–1022.
Draper, K., Ponsford, J., 2008. Cognitive functioning ten years following traumatic brain injury and rehabilitation. Neuropsychology 22, 618–625.
Draper, K., Ponsford, J., Schönberger, M., 2007. Psychosocial and emotional outcomes 10 years following traumatic brain injury. J. Head Trauma Rehabil. 22, 278–287.
Fagerholm, E.D., Hellyer, P.J., Scott, G., Leech, R., Sharp, D.J., 2015. Disconnection of network hubs and cognitive impairment after traumatic brain injury. Brain 138, 1696–1709.
Fornito, A., Zalesky, A., Breakspear, M., 2015. The connectomics of brain disorders. Nat. Rev. Neurosci. 16, 159–172.
Fox, M.D., Greicius, M., 2010. Clinical applications of resting state functional connectivity. Front. Syst. Neurosci. http://dx.doi.org/10.3389/fnsys.2010.00019.
Fransson, P., Marrelec, G., 2008. The precuneus/posterior cingulate cortex plays a pivotal role in the default mode network: evidence from a partial correlation network analysis. NeuroImage 42, 1178–1184.
Friston, K.J., Holmes, A.P., Worsley, K.P., Poline, J.B., Frith, C.D., Frackowiak, R.S., 1995. Statistical parametric maps in functional imaging: a general linear approach. Hum. Brain Mapp. 2, 189–210.
Greenacre, M.J., 1983. Theory and Applications of Correspondence Analysis. Academic Press, London.
Greenspan, L., McLellan, B.A., Greig, H., 1985. Abbreviated injury scale and injury severity score: a scoring chart. J. Trauma 25, 60–64.
Greicius, M.D., Kiviniemi, V., Tervonen, O., Vainionpää, V., Alahuhta, S., Reiss, A.L., Menon, V., 2008. Persistent default-mode network connectivity during light sedation. Hum. Brain Mapp. 29, 839–847.
Ham, T.E., Sharp, D.J., 2012. How can investigation of network function inform rehabilitation after traumatic brain injury? Curr. Opin. Neurol. 25, 662–669.
Hermann, M., Jost, S., Kutz, S., Ebert, A.D., Kratz, T., Wunderlich, M.T., Synowitz, H., 2000. Temporal profile of release of neurobiochemical markers of brain damage after traumatic brain injury is associated with intracranial pathology as demonstrated in cranial computerized tomography. J. Neurotrauma 17, 113–122.
Hillary, F.G., Slocomb, J., Hills, E.C., Fitzpatrick, N.M., Medaglia, J.D., Wang, J., Wylie, G.R., 2011. Changes in resting connectivity during recovery from severe traumatic brain injury. Int. J. Psychophysiol. 82, 115–123.
Himanen, L., Portin, R., Isoniemi, H., Helenius, H., Kurki, T., Tenovuo, O., 2006. Longitudinal cognitive changes in traumantic brain injury: a 30-year follow-up study. Neurology 66, 187–192.
Hukkelhoven, C.W., Steyerberg, E.W., Rampen, A.J., Farace, E., Habbema, J.D., Marshall, L.F., Murray, G.D., Maas, A.I., 2003. Patient age and outcome following severe traumatic brain injury: an analysis of 5600 patients. J. Neurosurg. 99, 666–673.
Husson, E.C., Ribbers, G.M., Willemse-van Son, A.H., Verhagen, A.P., Stam, H.J., 2010. Prognosis of six-month functioning after moderate to severe traumatic brain injury: a systematic review of prospective cohort studies. J. Rehabil. Med. 42, 425–436.
Ingebrigtsen, T., Romner, B., Kongstad, P., Langbakk, B., 1995. Increased serum concentrations of protein S-100 after minor head injury: a biochemical serum marker with prognostic value? J. Neurol. Neurosurg. Psychiatry 59, 103–104.
Iraji, A., Benson, R.A., Welch, R.D., O'Neil, B.J., Woodard, J.L., Ayaz, S.I., Kulek, A., Mika, V., Medado, P., Soltanian-Zadeh, H., Liu, T., Haacke, E.M., Zhifeng, Z., 2015. Resting state functional connectivity in mild traumatic brain injury at the acute stage: independent component and seed-based analysis. J. Neurotrauma 32, 1031–1045.
Irima, A., Wang, B., Aylward, S.R., Prastawa, M.W., Pace, D.F., Gerig, G., Hovda, D.A., Kikinis, R., Vespa, P.M., Van Horn, J.D., 2012. Neuroimaging of structural pathology and connectomics in traumatic brain injury: toward personalized outcome prediction. NeuroImage Clin. 1, 1–17.
Jennett, B., 1996. Epidemiology of head injury. J. Neurol. Neurosurg. Psychiatry 60, 362–369.
Jennett, B., Bond, M., 1975. Assessment of outcome after severe brain damage. Lancet 1, 480–484.
Kasahara, M., Menon, D.K., Salmond, C.H., Outtrim, J.G., Taylor Tavares, J.V., Carpenter, T., Stamatakis, E.A., 2010. Altered functional connectivity in the motor network after traumatic brain injury. Neurology 75, 168–176.
Lorenzo-Seva, U., van de Velden, M., Kiers, H.A.L., 2009. CAR: a Matlab package to compute correspondence analysis with rotations. J. Stat. Softw. 31, 8.
Maas, A.I., Hukkelhoven, C.W., Marshall, L.F., Steyerberg, E.W., 2005. Prediction of outcome in traumatic brain injury with computed tomographic characteristics: a comparison between the computed tomographic classification and combinations of computed tomographic predictors. Neurosurgery 57, 1173–1182.
Marmarou, A., Lu, J., Butcher, I., McHugh, G.S., Murray, G.D., Steyerberg, E.W., Mushkudiani, N.A., Choi, S., Maas, A.I., 2007. Prognostic value of the Glasgow coma scale and pupil reactivity in traumatic brain injury assessed pre-hospital and on enrollment: an IMPACT analysis. J. Neurotrauma 24, 270–280.
Martins, E.T., Linhares, M.N., Sousa, D.S., Schroeder, H.K., Meinerz, J., Rigo, L.A., Bertotti, M.N., Gullo Jm Hohl, A., Dal-Pizzol, F., Walz, R., 2009. Mortality in severe traumatic brain injury: a multivariated analysis of 748 Brazilian patients from Florianópolis City. J. Trauma 67, 85–90.
Mayer, A.R., Ling, J.M., Allen, E.A., Klimaj, S.D., Yeo, R.A., Hanlon, F.M., 2015. Static and dynamic intrinsic connectivity following mild traumatic brain injury. J. Neurotrauma 32, 1046–1055.
Mercier, E., Boutin, A., Lauzier, F., Fergusson, D.A., Simard, J.F., Zarychanski, R., Moore, L., McIntyre, L.A., Archambault, P., Lamontagne, F., Légaré, F., Randell, E., Nadeau, L., Rousseau, F., Turgeon, A.F., 2013. Predictive value of S-100β protein for prognosis in patients with moderate and severe traumatic brain injury: systematic review and meta-analysis. BMJ http://dx.doi.org/10.1136/bmj.f1757.
Miller, H., 1966. Mental after-effects of head injury. Proc. R. Soc. Med. 59, 257–261.
Miller, J.D., Butterworth, J.F., Gudeman, S.K., Faulkner, J.E., Choi, S.C., Selhorst, J.B., Harbison, J.W., Lutz, H.A., Young, H.F., Becker, D.P., 1981. Further experience in the management of severe head injury. J. Neurosurg. 54, 289–299.

Miller, K.J., Schwab, K.A., Warden, D.L., 2005. Predictive value of an early Glasgow outcome scale score: 15-month score changes. J. Neurosurg. 103, 239–245.
Moen, K.G., Brezova, V., Skandsen, T., Håberg, A.K., Folvik, M., Vik, A., 2014. Traumatic axonal injury: the progonstic value of lesion load in corpus collosum, brain stem, and thalamus in different magnetic resonance imaging sequences. J. Neurotrauma 31, 1486–1496.
Murray, G.D., Butcher, I., McHugh, G.S., Lu, J., Mushkudiani, N.A., Maas, A.I., Marmarou, A., Steyerberg, E.W., 2007. Multivariable prognostic analysis in traumatic brain injury: results from the IMPACT study. J. Neurotrauma 24, 329–337.
Mushkudiani, N.A., Engel, D.C., Steyerberg, E.W., Butcher, I., Lu, J., Marmarou, A., Slieker, F., McHugh, G.S., Murray, G.D., Maas, A.I., 2007. Prognostic value of demographic characteristics in traumatic brain injury: results from the IMPACT study. J. Neurotrauma 24, 259–269.
Nakamura, T., Hillary, F.G., Biswal, B.B., 2009. Resting network plasticity following brain injury. PLoS One 4, e8220.
Pandit, A.S., Expert, P., Lambiotte, R., Bonnelle, V., Leech, R., Turkheimer, F.E., Sharp, D.J., 2013. Traumatic brain injury impairs small-world topology. Neurology 80, 1826–1833.
Pleines, U.E., Morganti-Kossmann, M.C., Rancan, M., Joller, H., Trentz, O., Kossmann, T., 2001. S-100beta reflects the extent of injury and outcome, whereas neuronal specific enolase is a better indicator of neuroinflammation in patients with severe traumatic brain injury. J. Neurotrauma 18, 491–498.
Power, J.D., Barnes, K., Snyder, A.Z., Schlaggar, B.L., Petersen, S.E., 2012. Spurious but systematic correlations in functional connectivity MRI networks arise from subject motion. NeuroImage 59, 2142–2154.
Raabe, A., Grolms, C., Sorge, O., Zimmermann, M., Seifert, V., 1999. Serum S-100B protein in severe head injury. Neurosurgery 45, 477–483.
Raabe, A., Kopetsch, O., Woszczyk, A., Lang, J., Gerlach, R., Zimmerman, M., Seifert, V., 2004. S-100B protein as a serum marker of secondary neurological complications in neurocritical care patients. Neurol. Res. 26, 440–445.
Ross, S.E., Leipold, C., Terregino, C., O'Malley, K.F., 1998. Efficacy of the motor component of the Glasgow coma scale in trauma triage. J. Trauma 45, 42–44.
Scheid, R., Preul, C., Gruber, O., Wiggins, C., von Cramon, D.Y., 2003. Diffuse axonal injury associated with chronic traumatic brain injury: evidence from T2*-weighted gradient echo imaging at 3T. Am. J. Magn. Reson. B. 24, 1049–1056.
Schrouff, J., Perlberg, V., Boly, M., Marrelec, G., Boveroux, P., Vanhaudenhuyse, A., Bruno, M.A., Laureys, S., Philips, C., Pelegrini-Issac, M., Maquest, P., Benali, H., 2011. Brain functional integration decreases during propofol-induced loss of consciousness. NeuroImage 57, 198–205.
Sehgal, V., Delproposto, Z., Haacke, E.M., Tong, K.A., Wycliffe, N., Dk, K., Xu, Y., Neelavalli, J., Haddar, D., Reichenbach, J.R., 2005. Clinical applications of neuroimaging with susceptibility-weighted imaging. J. Magn. Reson. Imaging 22, 439–450.
Sharp, D.J., Beckmann, C.F., Greenwood, R., Kinnunen, K.M., Bonnelle, V., De Boissezon, X., Leech, R., 2011. Default mode network functional and structural connectivity after traumatic brain injury. Brain 134, 2233–2247.
Sharp, D.J., Scott, G., Leech, R., 2014. Network dysfunction after traumatic brain injury. Nat. Rev. Neurol. 10, 156–166.
Shumskaya, E., Andriessen, T.M., Norris, D.G., Vos, P.E., 2012. Abnormal whole-brain functional networks in homogeneous acute mild traumatic brain injury. Neurology 79, 175–182.
Stocchetti, N., Pagan, F., Calappi, E., Canavesi, K., Beretta, L., Cirerio, G., Cormio, M., Colombo, A., 2004. Inaccurate early assessment of neurological severity in head injury. J. Neurotrauma 21, 1131–1140.
Tate, R.L., Godbee, K., Sigmundsdottir, L., 2013. A systematic review of assessment tools for adults used in traumatic brain injury research and their relationship to the ICF. NeuroRehabilitation 32, 729–750.
Teasdale, G., Jennett, B., 1976. Assessment of coma and impaired consciousness. A practical scale. Lancet 13, 81–84.
Teasdale, G.M., Pettigrew, L.E., Wilson, J.T., Murray, G., Jennett, B., 1998. Analyzing outcome of treatment of severe head injury: a review and update on advancing the use of the Glasgow outcome scale. J. Neurotrauma 15, 587–597.
Temkin, N.R., Corrigan, J.D., Dikmen, S.S., Machamer, J., 2009. Social functioning after traumatic brain injury. J. Head Trauma Rehabil. 24, 460–467.
Thelin, E.P., Johannesson, L., Nelson, D.W., Bellander, B.M., 2013. S100B is an important outcome predictor in traumatic brain injury. J. Neurotrauma 30, 519–528.
Thelin, E.P., Nelson, D.W., Bellander, B.M., 2014. Secondary peaks of S100B in serum relate to subsequent radiological pathology in traumatic brain injury. Neurocrit. Care. 20, 217–229.
Thelin, E.P., Zibung, E., Riddez, L., Nordenvall, C., 2015. Assessing bicycle-related trauma using the biomarker S100B reveals a correlation with total injury severity. Eur. J. Trauma Emerg. Surg. (2015 Oct 21).
Tzourio-Mazoyer, N., Landeau, B., Papathanassiou, D., Crivello, F., Etard, O., Delcroix, N., Mazoyer, B., Joliot, M., 2002. Automated anatomical labeling of activations in SPM using a macroscopic anatomical parcellation of the MNI MRI single-subject brain. NeuroImage 15, 273–289.
Undén, J., Ingebrigtsen, T., Romner, B., Scandinavian Neurotrauma Committee (SNC), 2013. Scandinavian guidelines for initial management of minimal, mild and moderate head injuries in adults: an evidence and consensus-based update. BMC Med. http://dx.doi.org/10.1186/1741-7015-11-50.
van Zomeren, A., van den Burg, W., 1985. Residual complaints of patients two years after severe head injury. J. Neurol. Neurosurg. Psychiatry 48, 21–28.
Vos, P.E., Jacobs, B., Andriessen, T.M.J.C., Lamers, K.J.B., Borm, G.F., Beems, T., Edwards, M., Rosmalen, C.F., Vissers, J.L.M., 2010. GFAP and S100B are biomarkers of traumatic brain injury: an observational cohort study. Neurology 75, 1786–1793.
Whitfield-Gabrieli, S., Nieto-Castanon, A., 2012. Conn: a functional connectivity toolbox for correlated and anti-correlated brain networks. Brain Connect. 2, 125–141.
Whitfield-Gabrieli, S., Ghosh, S.S., Nieto-Castanon, A., Saygin, Z., Doehrmann, O., Chai, X.J., Reynolds, G.O., Hofmann, S.G., Pollack, M.H., Gabrieli, J.D.E., 2015. Brain connectomics predict response to treatment in social anxiety disorder. Mol. Psychiatry 1–6.
Wintermark, M., Sanelli, P.C., Anzai, Y., Tsiouris, A.J., Whitlow, C.T., ACR Head Injury Institute, 2015. Imaging evidence and recommendation for traumatic brain injury: conventional neuroimaging techniques. J. Am. Coll. Radiol. 12, e1–e14.
Yarkoni, T., Poldrack, R.A., Nichols, T.E., van Essen, D.C., Wager, T.D., 2011. Large-scale automated synthesis of human functional neuroimaging data. Nat. Methods 8, 665–670.
Yokobori, S., Hosein, K., Burke, S., Sharma, I., Gajavelli, S., Bullock, R., 2013. Biomakers for clinical differential diagnosis in traumatic brain injury – a systematic review. CNS Neurosci. Ther. 19, 556–565.